



OPEN

Solubility of vitamin A in supercritical CO₂: experimental study and thermodynamic modeling

Gowhar Ahmad Naikoo^{1,6}, Mohammad Saeedi Zadegan^{2,6}, Mona Zamani Pedram²✉, Israr Ul Hassan³, Waqar Ahmed⁴ & Golshan Yousefi Attar⁵

One of the best methods of extracting Vitamin A, as a helper of the immune body system and vision, was measured in supercritical carbon dioxide (SC-CO₂); Mole fractions were gained at practical conditions in which the temperature was in the range of 303–323 K and the pressure range was 90–235 bar, respectively. Moreover, four Equation of States [Soave–Redlich–Kwong, Peng–Robinson, Stryjek–Vera and Dashtizadeh–Pazuki–Taghikhani–Ghotbi (DPTG)] were compared with the experimental data. Also, the mixing rules of Van der Waals (vdW1 and vdW2) selected to correlate the solubility data of vitamin A. The outcomes indicate that each of EOSs coupled with vdW2, as a method of estimating the physicochemical and critical properties, were correlated with the solubility data of vitamin A in SC-CO₂ with more accuracy, in comparison with vdW1. Among the cubic EOSs, the DPTG model with vdW2 generated the most suitable correlation with the percentage average absolute relative deviation (Average Absolute Relative Deviation%) of 6.

List of symbols

a(T)	Energy parameter of in the cubic EOS (Nm ⁴ mol ⁻²)
b	Parameter depend on Volume in cubic Equations-Of-State (m ³ mol ⁻¹)
E	Solubility enhancement factor
EOS	Equation-Of-State
k_{ij}, l_{ij}	Mixing rule (binary interactions)
N	Experimental points
P	Density (kg m ⁻³)
P	Pressure (Pa)
R	Universal gas constant (J mol ⁻¹ K ⁻¹)
SRK	Soave–Redlich–Kwang
V	Molar volume (m ³ mol ⁻¹)
vdW1	Van der Waals mixing rule with one adjustable parameter
vdW2	Van der Waals mixing rule with two adjustable parameters
y	Mole fraction solubility
k1	Pure compound adjustable parameters

Greek symbols

$\alpha(T_r, \omega)$	Function in the attractive parameter of the EOS's
ω	Pitzer's acentric factor

¹Department of Mathematics and Sciences, College of Arts and Applied Sciences, Dhofar University, Salalah 211, Sultanate of Oman. ²Faculty of Mechanical Engineering-Energy Division, K.N. Toosi University of Technology, No. 15-19, Pardis St., Mollasadra Ave., Vanak Sq., P.O. Box 19395-1999, 1999 143344 Tehran, Iran. ³College of Engineering, Dhofar University, Salalah 211, Sultanate of Oman. ⁴School of Mathematics and Physics, College of Science, University of Lincoln, Lincoln LN6 7TS, UK. ⁵Department of Chemical engineering, Islamic Azad University south Tehran Branch, Tehran, Iran. ⁶These authors contributed equally: Gowhar Ahmad Naikoo and Mohammad Saeedi Zadegan. ✉email: m.zpedram@kntu.ac.ir

Subscripts

1	Supercritical solvent
A	Vitamin A
C	Critical property
<i>cal</i>	Calculated mode
<i>exp</i>	Experimental mode
<i>i, j</i>	Components

Superscripts

s	Solid (vitamin A)
sub	In sublimation
SCF	In supercritical phase

Despite extensive research on the knowledge and importance of Vitamin A^{1,2} in the human body, the process of extracting and producing these materials from natural sources is not easy. Also, Vitamin A is soluble only in non-polar solvents due to having a bond O–H to the whole molecule (Table 1). In addition to this constraint, the operating conditions including temperature, pressure, exposure to air, light, moisture, water activity and pH are considerably affected by them which affects the characterization tests or equipment into practice which have to operate within permissible operating conditions³. Hence, separation and purification of natural vitamins can be identified as an optimum and economic step to produce pharmaceutical solids and reduce the side effects of synthetic ones⁴. Fortunately, extraction with supercritical fluid is a helpful method for purification of sensitive medicines from natural sources.

In fact, supercritical fluid extraction (SFE) is referred to a process in which one the extracting component is separated from another by means of fluids which are supercritical. Hence, these supercritical fluids were applied as the extracting solvent. In consequence they pave the way to mildly and selectively isolate substances from natural material^{4–6}. This technology contributed to achieve extracts which are superior from a quality point of view with higher yield. Notably, there is no residual solvent. The SFE technique holds various features such as higher extraction efficiencies, simple and easy separation technology, no need for solvent recovery equipment and completion near to standard room temperature conditions⁷.

In this way, one of the best solvents amid them is SC-CO₂ that is obtainable at high purities and low cost with low critical temperature and pressure (TC = 304.18 K and PC = 73.8 bar) and small surface tension as well as high selectivity⁸. Moreover, no residual solvent is detected by extract products taken from SC-CO₂. Notably, this procedure is seductive to the food and beverage and medical industries. In comparison with other procedures, it brings about the least harm to the environment. CO₂ has been labelled as the namely "green" solvent by the Federal Drug Administration (FDA), which is safe for industrial extractions⁹.

In this way, it is significant to determine the solubility of vitamins in supercritical phase (SCF). Such determination is suitable to design and develop the pharmaceutical processes; the computation and thermodynamic modeling should predict them¹⁵. Considerably, it is economically interesting to know the characteristic of phase equilibrium to optimize computation of separation processes.

One of the essential and significant approaches is modeling of solubility parameter in the SCF through EOS-based models with varied mixing rules, mathematically. This method is mainly employed to calculate phase equilibrium of neat fluids and mixtures as well as thermodynamic properties^{10–12}. Also, to assess the solute solubility in supercritical fluid, the most pertinent models are the quadratic van der Waals equations of state as the most applicable models. These equations have been identified as the suitable ones which are able to estimate fluid phase equilibrium¹³.

Furthermore, a number of critical, physical and chemical properties are needed for several current models. It should be noted that such properties of solid hold critical sublimation pressure, Pitzer acentric feature and critical properties although they have never been achieved from an experimental point of view. Indeed, the consequential errors for different models are achieved; arising from the estimation method of the critical, physical, and chemical properties¹⁴.

The strengths and constraints of the employed equations of states are the two important factors which are able to develop a desirable mathematical model. As a result, this model is employed to estimate the solubility parameter in supercritical fluids.

Afterward, it is essential to precisely evaluate the use of reliable mixing rules which can predict the phase equilibrium. As a result, several researchers have confirmed the two-parameter van der Waals mixing rule displays the suitable ability to conclude the behavior of phase equilibria in nonpolar compounds or the ones with low polarity^{15,16}. Recently, to predict the behavior of high polar materials with inherent deviation from the ideal condition, new mixing rules have been propounded.

The aforementioned equations (including SRK¹⁷, PR¹⁸, SV¹⁹ and DPTG²⁰ with two adjustable parameters are performed in order to correlate the experimental data) with the solubility parameter can be measured and evaluated the predicted results with respect to the performed modification.

In addition, the EOSs selected in this work, have been chosen because of their special features which are completely attempted to the solubility extraction about vitamins. In other words, there are common properties between these equations include^{17–20}:

- Ability to calculate to establish the relationship between temperature, pressure and volume of gases in supercritical situations.

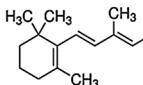
Name compound	Chemical formula	Structure	MW (g/mol)	λ_{max} (nm)	CAS number	Minimum purity
Retinol	C ₂₀ H ₃₀ O		286.45	325	68-26-8	95%

Table 1. Molecular structure of vitamin A².

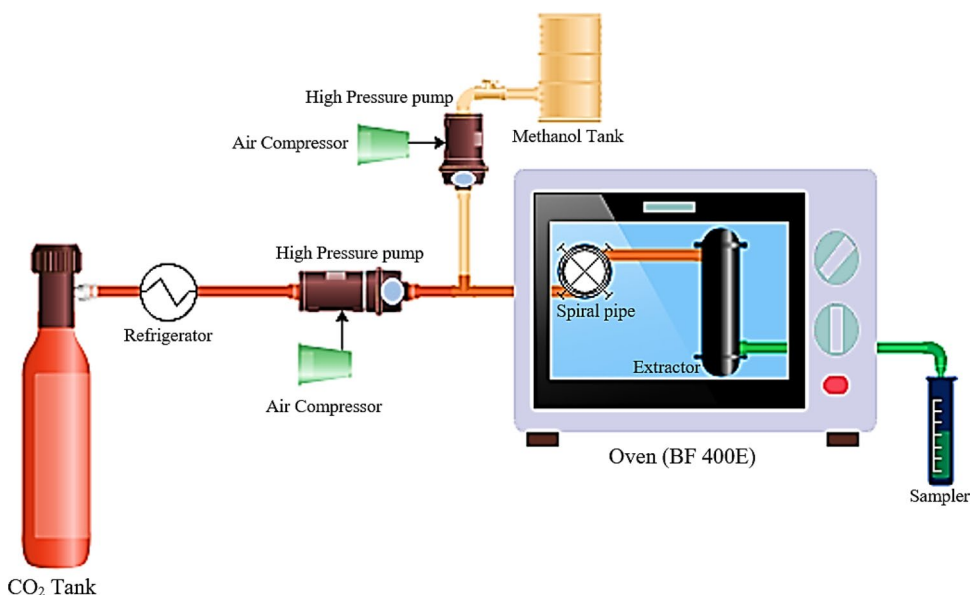


Figure 1. The setup shown schematic diagram of the experimental setup used for measuring solubility.

- predicting gas-phase properties of solubility compounds, in vapor–liquid equilibria.
- In this EOSs, the effect of intermolecular forces and size of molecules are considered.

In order to evaluate its ability and estimate the deviation from the ideal state, the two-parameter mixing rules of van der Waals are practiced. The experimental data under the anticipated operating conditions for the binary vitamin A-SC-CO₂ system was used.

The deviation of the calculated outcomes was calculated by the experimental data in order to evaluate the abilities of the selected models represented in terms of the AARD%. Moreover, the sublimation pressure is essential for the accuracy of the calculations which is anticipated to be used at the end of the calculations as a lever to validate the state equations.

In this work, a new study has been done for investigation the solubility points of vitamin A in supercritical solvent in two separate parts. In the first part (experimentally), the amount of molar fraction extracted by the setup designed (Setup description section) is recorded. In the second part (theoretically), these solubility points are compared with the calculated points by the EOS. Finally, total deviations between two numbers (experimental and calculations points) are investigated as a measure for select a more accurate EOS to predict the solubility points of vitamin A in the SC-CO₂ solution.

Methods

Materials. Zagrosgas Company (Tehran, Iran) supplied the carbon dioxide (CO₂) (CAS Number 124-38-9) at a least clarity of 99.99%. Retinol (Vitamin A) (CAS Number 68-26-8) with purity (GC) >95% was obtained from Safirazma (Tehran, Iran). Also, analytical grade methanol (CAS Number 67-56-1) with purity of 99.8% was purchased from Safirazma (Tehran, Iran).

Setup description. Figure 1 indicates the system used for measuring the equilibrium solubility. Before it was introduced into the fridge, the CO₂ gas was passed through the pump by means of revealing the valve on a stainless-steel flask. Consequently, the gas was liquefied through dropping the temperature to -20 °C so that it was prepared for pumping function by means of pressure controlling instruments (TEBCO, Iran) with an uncertainty of ±0.1 MPa.

After CO₂ pumped into the inlet solvent stream, the methanol tank (as a co-solvent in this section) and modulator valve controlled the solvent concentration. The inlet solvent concentration should be regulated. Thus, it is an adjustable factor as function of solute content based on simultaneous data from experimental setup. The pressure of the circuit was taken into the collection container through altering amount of modulator on the injection tap. This includes a certain volume of solvent (CO₂ and methanol). Providing the thermal equilibrium condition with the inner part of the oven in shorter time, this equilibrium spiral pipe can be utilized for efficient mixing of CO₂ and modulators. The cell was put inside carefully (FG Model, BF400E, Iran) to keep the operating temperature (with ± 0.5 K).

Roughly before the start of the extraction, 500 mg of powder Retinol were put into the static cell with the volume of 10 mL and due to the pressure drop, downward flowrate (in line with weight force of the materials) was used. Eluding physical entrainment of the unextracted Vitamin A (Rich Retinol), the tops of the pressurized equilibrium cell were connected by means of the stainless-steel disks before SC-CO₂ was distributed into the cell, its pressure was enhanced up to the anticipated pressure before it is moved through the equilibrium cell at operational conditions. In the present research, 60 min was estimated to achieve the state of equilibrium (in the cell). It was shown to be sufficient through basic experiments.

In fact, the final sample (in the standard state) in two phases of gas (carbon dioxide) and liquid phase (solution containing methanol and vitamin A) It was stored in accumulation glass and entered the spectrophotometer. Finally, the solvent was used to clean the circuit.

As solubility values of Vitamin A were obtained in various conditions, they were noted by absorbency measurement's at λ_{max} using a model 2100 UNICO UV-VIS spectrophotometer with 1000 nm Wavelength. The equilibrium mole fraction y_A and equilibrium solubility, $S(g/L)$ in SC-CO₂ over the ranges of temperature and pressure obtained from below equation²¹:

$$y_A = n_A / (n_A + n_C) \quad (1)$$

where

$$n_A = (C_A (g/L) \times V_A (L)) / (M_A (g/mol)) \quad (2)$$

$$n_C = (V_1 (L) \times \rho (g/L)) / (M_C (g/mol)) \quad (3)$$

where n_A and n_C are sample moles of vitamin A and solvent, C_A is the concentration of vitamin A (g/L) in the accumulation glass calculated by the curve of calibration. The volumes of the accumulation vial are denoted by $V_A(L)$ and $V_1(L)$ is the sampling circuit. Furthermore, M_A and M_C are the molecular weights of Vitamin A and CO₂, respectively. By combining the aforementioned, the subsequent relation is achieved (Eq. (4)).

$$y_A = \frac{C_A \left(\frac{g}{L}\right) \times V_s(L) \times M_C \left(\frac{g}{mol}\right)}{C_A \left(\frac{g}{L}\right) \times V_A(L) \times M_C \left(\frac{g}{mol}\right) + V_1(L) \times \rho \left(\frac{g}{L}\right) \times M_A \left(\frac{g}{mol}\right)} \quad (4)$$

In order to obtain the (g/L) of Vitamin A in SC-CO₂ Eq. (4) was used²¹.

$$S(g/L) = (C_A (g/L) \times V_A (L)) / (V_1 (L)) \quad (5)$$

Sublimation pressure estimation. Using supercritical solvents is considered as a new method in the purification process of pharmaceutical solids. When the solubility reliance on pressure and temperature is explicitly defined, it is possible to optimize the supercritical extraction. Notably, one of the significant design parameters is detected to be the sublimation pressure in the industrial solid-liquid separation processes.

In the present research, by means of the Clapeyron relation joined from the triple point pressure P_t and temperature T_t , the sublimation pressure P^s at a temperature T is assessed with assuming an insignificant functionality of the sublimation enthalpy to temperature²²:

$$\ln(P^s/P_t) = - (\Delta H^s) / R(1/T - 1/T_t) \quad (6)$$

In which, ΔH^s presents the sublimation enthalpy at the triple point which can be analyze by the equation below due the singularity of the triple point²³.

$$\Delta H^s = \Delta H^v + \Delta H^f \quad (7)$$

In which ΔH^f and ΔH^v are the fusion enthalpies and vaporization at the triple point, correspondingly. In many conditions, the triple point conditions are indefinite experimentally and the use of (Eqs. (1) and (2)) only needs some specific thermodynamic conditions. The method planned with this is established in two stages. Initially, it is supposed that the triple point temperature T_t can be assessed by $DinT$ of the normal fusion temperature T_f . Certainly, the experimental values of transition temperatures in various literatures are scattered less than 0.1 K which is the difference between these two temperatures for the majority of heavy compounds²⁴.

Based on this assumption, ΔH^f in (Eq. (6)) can be projected by the synthesis enthalpy measured at the normal boiling point, thus application of Eq. (5) just needs specifying of Pt and ΔH^v at this temperature. In the next step, a correlation of vapor pressures is used to compute Pt and ΔH^v In this situation, experimental values of P^{sat} are first interrelated through a relation due to temperature. In the current research, experimental statement of the vapor pressure applied²⁵.

$$\ln(P^{sat}) = A + B/(T + C) + DinT + ET \quad (8)$$

In which bounds A, B, C, D, E were adjusted with the practical data. The equation of Yaws was used to obtain this statement in the case that very limited data points are available²⁶.

Let subscript C stand for the light (SC-CO₂) component and let subscript A stands for the heavy (Vitamin A) component. First, the general equation of equilibrium for Vitamin A at distinct operating conditions is written to calculate the solubility in the gas phase.

$$f_A^s = f_A^{SCF} \quad (9)$$

In which, superscript S characterizes the solid state. In this study, the supercritical fluid is presumed to not to be soluble in the solute stage. Additionally, the molar volume of the solute is pressure-independent and at sublimation point, the solute fugacity coefficient equals to 1. Solid phase is incompressible and pure. By considering the aforementioned assumptions, the derivation of equations is performed as following:

$$f_A^s = P_A^{sub} \phi_A^{sub} \exp\left(\int_{P_A^{sub}}^P \frac{V_A^s dP}{RT}\right) \quad (10)$$

where P_A^{sub} is the sublimation pressure, ϕ_A^{sub} is the fugacity coefficient at sublimation pressure point, and V_A^s is the solid molar volume, all at temperature T . For the fugacity of vapor-phase, we present fugacity coefficient ϕ_A^{sub} through eliciting its explanation.

$$f_A^{SCF} = P y_A \phi_A^{SCF} \quad (11)$$

We achieve the anticipated solubility of the heavy component in the gas phase by replacing and solving for y_A :

$$y_A = \left(\frac{P_A^{sub}}{P}\right) / P \times E \quad (12)$$

where

$$E = \frac{\phi_A^{sub} \exp\left(\int_{P_A^{sub}}^P \frac{V_A^s dP}{RT}\right)}{\phi_A^{SCF}} = \frac{\phi_A^{sub} \exp\left(\frac{V_A^s (P - P_A^{sub})}{RT}\right)}{\phi_A^{SCF}} \quad (13)$$

The enhancement factor E comprises three correction terms. The first term is the Poynting factor showing the effect of pressure on the pure solid fugacity which is considerable for the case of enhancement factor less than 2 or 3. The next correction, ϕ_A^{sub} , considers non-ideality of the pure saturated vapor; the sublimation pressure of the solid is very small leading ϕ_A^{sub} to be almost equal to unity in most applied cases. The final term, ϕ_A^{SCF} , is the last but the most significant. Nevertheless, ϕ_A^{SCF} is always far from unity and can yield great enhancement factors.

With the given numerical value of the y_A parameter from previous experimental data, we can calculate the sublimation pressures at those conditions (Eq. (11)). Moreover, with this new data points about the sublimation pressure and the EOSs, we can predict new data points about solubility mole fractions (y_A).

In fact, this fulfills the fugacity equation (Eq. (8)) and it is essential to measure the solution to the fugacity equation to confirm the minimum Gibbs energy or since fugacity is needed for an adequate condition for a steady equilibrium¹⁰. As the temperatures, at which the solubility of Vitamin A was examined (303, 313 and 323 K), are well underneath its melting point, it is not necessary do a thermodynamic constancy analysis. Evidently, none of the considered temperatures are very close to the critical point of CO₂ and they are amid the lower and upper critical end point.

To calculate ϕ_A^{SCF} we used different EOS-based models as described in later section. Consequently, we conclude an exclusive thermodynamically solution to the fugacity condition at each T and P allocating to the stable solid–fluid equilibrium²⁷. The values for critical parameters, acentric factor, and sublimation pressure of Vitamin A should be put on Eq. (11) in order to calculate the solubility. Afterwards, we practice diverse EOS-based models for estimation of ϕ_A^{SCF} .

Equation of state-based models. According to the thermodynamic models mentioned in the previous sections, now they are examined in more detail. As already stated, the SRK¹⁷, PR¹⁸, SV¹⁹ and DPTG²⁰ EOSs have been employed to calculate the fugacity constants in order to conclude the solubility of Vitamin A in SC-CO₂ accompanied with relating vdW1 and vdW2 mixing rules (supplementary for more detail).

Historically, cubic equations of state like (RK (and SRK), PR, SV and DPTG)^{17–20} are identified as the best choice modeling for phase equilibrium computations for multicomponent mixtures.

Moreover, it is required to conduct research so that the analytical cubic equations of state can be entirely developed. In this regard, improving the temperature dependency of attraction terms and the $P(v)$ functional form so as to control the vapor pressure (estimation and enhance the prediction of volumetric properties are the main development of this study.

Based on perturbation theory, a new two-parameter cubic equation of state is suggested.

In the meantime, DPTG equation of state²⁰ are used for the sake of precise calculation of the solubility factor since the outstanding role of solubility parameter has a significant consequence on the results of the model. Furthermore, the exactness of this EOS has been deliberated through estimation of the solubility in some

supercritical fluids like CO₂, methane and condensate gases, vaporization etc. Regarding previous studies^{36–37}, the corresponding fluid phase behavior in both subcritical and supercritical fluid areas can be reliably foretold that the DTGP²⁰ equations of state could indicated this.

Compressibility fugacity. The fugacity coefficient of the system and component *i* that shown in equations below, ($\hat{\phi}$ and $\hat{\phi}_i$ respectively) are identified as the two types of fugacity coefficients in thermodynamics^{28,29}. In addition, $\ln \hat{\phi}_i$ and $\ln \hat{\phi}$ can be gained over the subsequent relation due to the functionality of fugacity coefficient and pressure:

$$\ln \hat{\phi}_i = \frac{1}{RT} \int_0^P \left(\bar{v}_i - \bar{v}_i^{ig} \right) dp = \int_0^P \left(\frac{\bar{v}_i}{RT} - \frac{1}{p} \right) dp \quad (14)$$

$$\ln \hat{\phi} = \frac{1}{RT} \int_0^P (v - v^{ig}) dp = \int_0^P \left(\frac{v}{nRT} - \frac{1}{p} \right) dp \quad (15)$$

Although the aforementioned approaches are really suitable in case the EOS for fluids is volume-explicit³⁰, this is not the case for pressure-explicit EOS (where P is a function of T, v, and x_i), such as the numerous cubic EOS and several non-cubic EOS. In such circumstances the independent P in Eqs. (14) and (15) should be distorted into v and this can be understood by means of the relations specified in the supplementary for more details.

$$\ln \hat{\phi}_i = -\frac{1}{RT} \int_{\infty}^{v_c} \left(\frac{\partial P}{\partial n_i} \right)_{T, v_c, n_j (j \neq i)} dv_i + \int_{\infty}^{v_c} \frac{1}{v_c} dv_c - \ln z \quad (16)$$

$$\ln \hat{\phi} = z - 1 - \ln z - \frac{1}{RT} \int_{\infty}^v \left(P - \frac{RT}{v} \right) dv \quad (17)$$

Meanwhile furthestmost EOS for fluids is pressure-explicit, Eq. (16) is more general than Eq. (14). Considering the component fugacity coefficients, most of the problems can be solved by the afore-said methods. Nonetheless, they bring about rough inadequacies. For instance, due to the intricated EOS in the first integral in Eq. (16) will be is problematic, or it cannot be recognized because the partial differentiation $(\partial P / \partial n_i)_{T, v_c, n_j (j \neq i)}$ which remarkably enhances the intricacy of integrated function. Necessarily, alternative approaches were taken in recent works³¹. Thus, they were easier than Eq. (16).

According to the previous studies $\ln \hat{\phi}_i$ can be derived from $\ln \hat{\phi}$ and also, A straight method for the derivation of $\ln \hat{\phi}_i$ from $\ln \hat{\phi}$ comes from the following relation³¹:

$$\ln \hat{\phi}_i = \left[\frac{\partial (n \ln \hat{\phi})}{\partial n_i} \right]_{T, P, n_j} \quad (18)$$

Solution procedure. The optimal evaluation of the global value of the model binary interaction parameter is performed in terms of using the mixing rules of vdW1 and vdW2. The mixing rules comprise of adjustable parameters to consider exact chemical bonding forces such as hydrogen bonding and interaction due to the various size of mixture constituents. Depending on the mole fractions of mixture components, these mixing rules are employed in order to reach the slightest error when the predictions of the EOSs are associated with practical data. The aforementioned factors are recognized as binary interaction parameter which are used as a scale for assessing the deviation from the behavior anticipated in non-ideal systems. At a certain temperature the binary interaction parameter is achieved through regressing the model against experimental data of Vitamin A solubility.

Figure 2 displays the stages needed so as to calculate the solubility. Furthermore, these stages indicate the several calculations done to calculate the solubility of Vitamin A in SC-CO₂ at different operating conditions.

The compatible function is the AARD% between the calculated and experimental solubility. In which N is the number of experimental points at each temperature. The whole relations concluding the equations of state as well as mixing rules practiced in this research are presented in the supplementary for more detail.

$$\text{AARD}(\%) = \frac{100}{N} \sum_{i=1}^N \frac{|y_{i,c} - y_{i,e}|}{y_{i,e}} \quad (19)$$

Result and desiccation

Experimental data. In this study when the pressure is in the range of 90–240 bar and the temperature range set at 303–323 K, equilibrium solubility data S (g/L) and the mole fraction (y) data of Vitamin A in SC-CO₂ were specified.

Table 2 features the outcomes. It is worth noting that all experiments were repeated three times so that accurate and precise measurements was ensured. Remarkably, the comparative normal uncertainties were less than 6%. Furthermore, Fig. 5 divulges the uncertainty associated with the each of EOS. (The Span-Wagner equation³² was applied to contribute the density of SC-CO₂. This equation is specifically formulated for CO₂). In this regard,

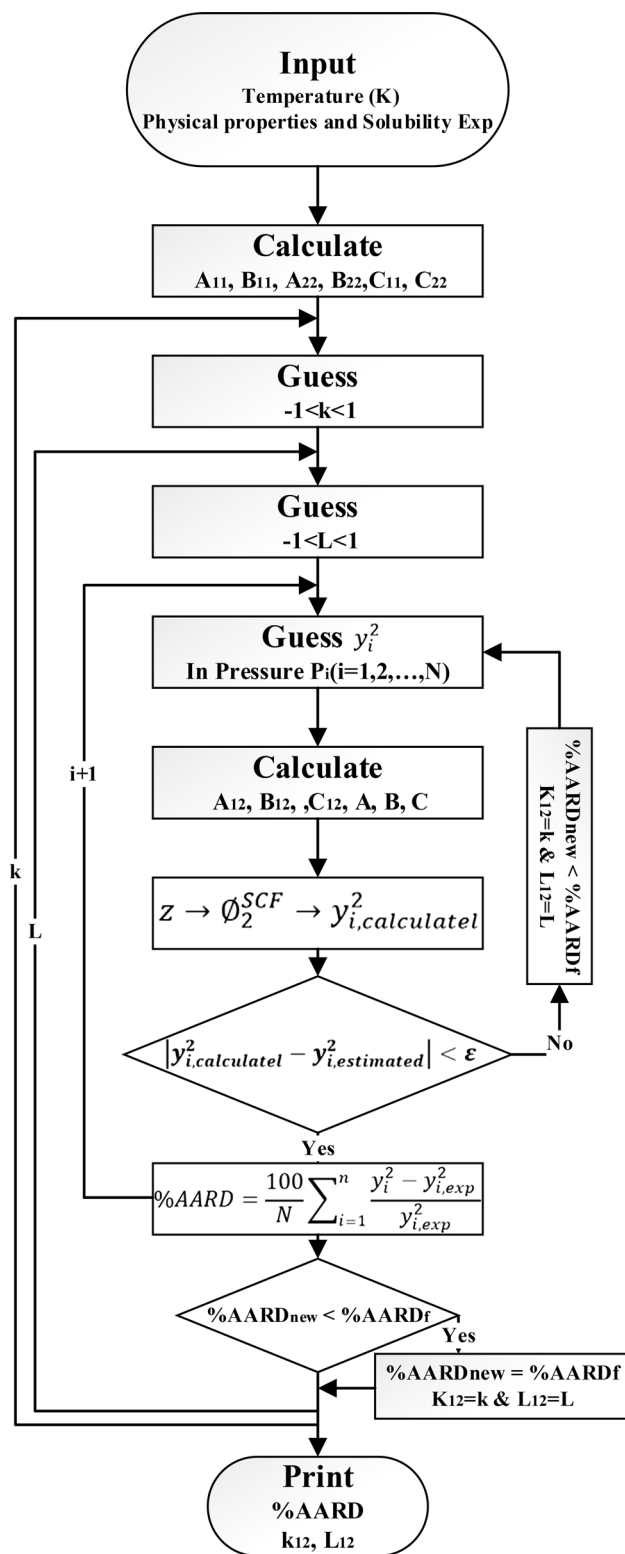


Figure 2. In the flowchart below, show the schematic of the calculations.

the mole fractions and solubility quantities of Vitamin A recorded varied from 2.18×10^{-5} to 1.964×10^{-4} and from 0.096 to 1.036, respectively. The maximum and minimum solubility of the Vitamin A were perceived at the temperature of 323 K and pressure of 235 bar and 303 K, 90 bar, correspondingly.

Temperature (K)	Pressure (bar)	Mole fraction ($\times 10^3$)	Density (g/l)	Solubility ($[\text{g/l}] \times 10^3$)
303	90	0.0218	681.6	96.74
303	115	0.0292	758.1	144.1
303	130	0.0358	789	183.9
303	140	0.0412	806.5	216.2
303	155	0.0529	829.3	285.5
303	175	0.0601	855.3	334.5
303	185	0.0625	866.9	352.7
303	195	0.0721	877.7	411.8
303	220	0.0796	901.9	467.2
303	230	0.0819	910.7	485.4
303	245	0.0832	923	499.8
313	100	0.0168	561.3	61.36
313	120	0.0362	664.1	156.5
313	130	0.0541	696.5	245.3
313	140	0.0525	723.2	247.1
313	155	0.0663	756.3	326.3
313	170	0.0813	783.8	414.8
313	200	0.1255	828.3	676.6
313	235	0.138	869.1	780.8
313	245	0.1492	879.2	854.0
323	110	0.0268	462.2	80.62
323	135	0.0524	603	205.6
323	165	0.1014	693	457.5
323	180	0.1402	725.3	661.9
323	195	0.1482	752.6	726.0
323	205	0.16	768.9	800.8
323	235	0.1964	810.5	1036

Table 2. Solubility of vitamin A in SC-CO₂ at various temperatures and pressures.

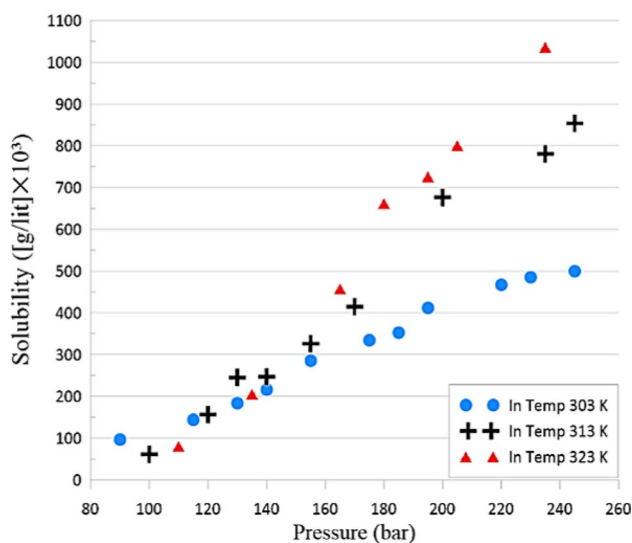


Figure 3. Solubility of Vitamin A vs pressure (at various temperatures).

According to Fig. 3, it can be deduced that solubility improves through increasing pressure at a constant temperature. This was brought about by the improved density along with the strong solvation property of SC-CO₂ at higher pressures. A double effect on solubility is detected by the temperature in SC-CO₂. This relies on in what way the solvent density and solute vapor pressure are well-adjusted^{34,35}. Indeed, increasing the solute vapor pressure might arise from the enhancement of the solution temperature.

EOS	Parameters	In 303.15 K	In 313.15 K	In 323.15 K
SRK-vdW1	k_{ij}	0.07979	0.119786	0.167963
	$P_{sub,2}$	5.76E-06	0.000165	0.003333
	AARD (%)	7.54	11.58	9.35
SRK-vdW2	k_{ij}	0.632664	0.538128	0.602364
	l_{ij}	0.585396	0.513787	0.592264
	$P_{sub,2}$	0.267549	0.114635	0.993638
	AARD (%)	5.67	3.64	3.81
PR-vdW1	k_{ij}	0.080396	0.116453	1.170893
	$P_{sub,2}$	1.04E-05	2.41E-05	0.004242
	AARD (%)	6.96	10.70	8.68
PR-vdW2	k_{ij}	0.181497	0.517322	0.583477
	l_{ij}	0.115645	0.491264	0.571054
	$P_{sub,2}$	6.29E-05	0.102111	0.889204
	AARD (%)	6.36	3.62	3.82
SV-vdW1	k_{ij}	0.092516	0.127765	0.171397
	$P_{sub,2}$	1.045047	3.81E-05	0.004141
	AARD (%)	6.96	10.68	8.66
SV-vdW2	k_{ij}	0.625796	0.522877	0.546006
	l_{ij}	0.581154	0.490355	0.504091
	$P_{sub,2}$	0.266842	0.100798	0.562166
	AARD (%)	5.68	3.62	3.97
DPTG-vdW1	k_{ij}	0.353399	0.325725	0.34744
	$P_{sub,2}$	0.050702	0.106757	0.691951
	AARD (%)	5.78	4.52	4.09
DPTG-vdW2	k_{ij}	0.353399	0.391577	0.364307
	l_{ij}	0.252096	0.110898	0.034643
	$P_{sub,2}$	0.050702	0.21614	0.778508
	AARD (%)	5.78	3.65	4.04

Table 3. Correlation results for solubility of vitamin A in SC-CO₂ solvent.

According to the Fig. 3, in pressure 110 bar, there is a cross-over pressure (at 303,313 and 323 K). This is despite the fact that in all cases, the solubility of vitamin A in SC-CO₂ was over than 0.15 g/lit.

Henceforth, it affects stronger solvating power of SCF. Simultaneously, it is recognized that the SC-CO₂ density might be diminished by a rise of temperature. This is detected to decline the total solvation property of the fluid.

Figure 3 indicates that the pressure range of 90–240 bar is in the beyond crossover pressure region for Vitamin A. Nonetheless, the density and solute vapor pressure are the leading factors at pressures under and beyond the crossover pressure region, correspondingly. For instance, the solubility may grow with temperature at pressures above the crossover pressure region. On the contrary to the 303 K which is recognized as the lowest one, the 323 K isotherm is highest isotherm. The solubility enhances through growing temperature for all pressures in the range examined. The behavior is influenced by two effects.

The primary is related with the increment of the solvating power of CO₂ for the sake of density and the other one is the enhancement of solubility according to lessening the vapor pressure of Vitamin A. In this regards, similar results have been reported by researchers in clarification of the binary effect of temperature on the solubility in SC-CO₂³³.

EOS-based models. As aforementioned, the EOS-based model was practiced in order to relate the solubility data of Vitamin A in SC-CO₂. Furthermore, the consequences were associated in terms of AARD%. To calculate the Vitamin A solubility in SC-CO₂, diverse combinations of EOSs such as the SRK¹⁷, the PR¹⁸, the SV¹⁹ and DPTG²⁰ with two mixing rules (VdW1 and VdW2) are put into practice.

At three operation temperatures (303, 313 and 323 K) the PR¹⁸ and SRK¹⁹ EOSs with mixing rules of vdW1 and vdW2 contributed to the correlation results (Table 3). The optimum binary interaction factors (k_{ij} and l_{ij}) as well as AARD% are held by them. The experimental data (27 data points) in extensive pressure at three levels of temperature were practiced to protect the generality of the current study.

Figure 4 indicates that less average absolute relative errors (5.77% at 303 K, 4.51% at 313 K and 4.09% at 323 K) can be obtained from the combination of DPTG EOS²⁰ along with applying vdW2 mixing rule. Definitely, it would be suitable for industrial uses. The deviations of the EOS-based models perhaps mostly owing to the point that cubic equations of state usually end to weak solubility predictions in supercritical fluid areas. In comparison with the results from other EOSs for this region, more reliable outcomes have been obtained from the DPTG EOS²⁰.

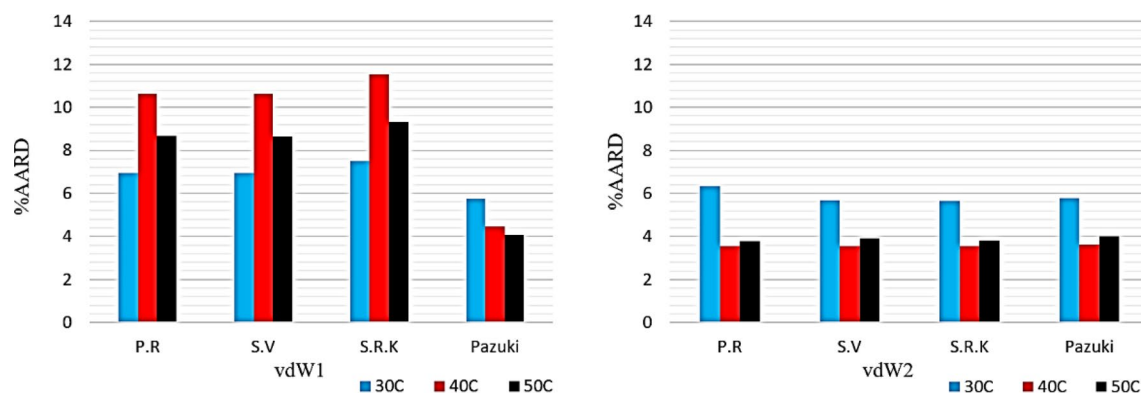


Figure 4. In the chart below shows the overall deviation of each of the models studied.

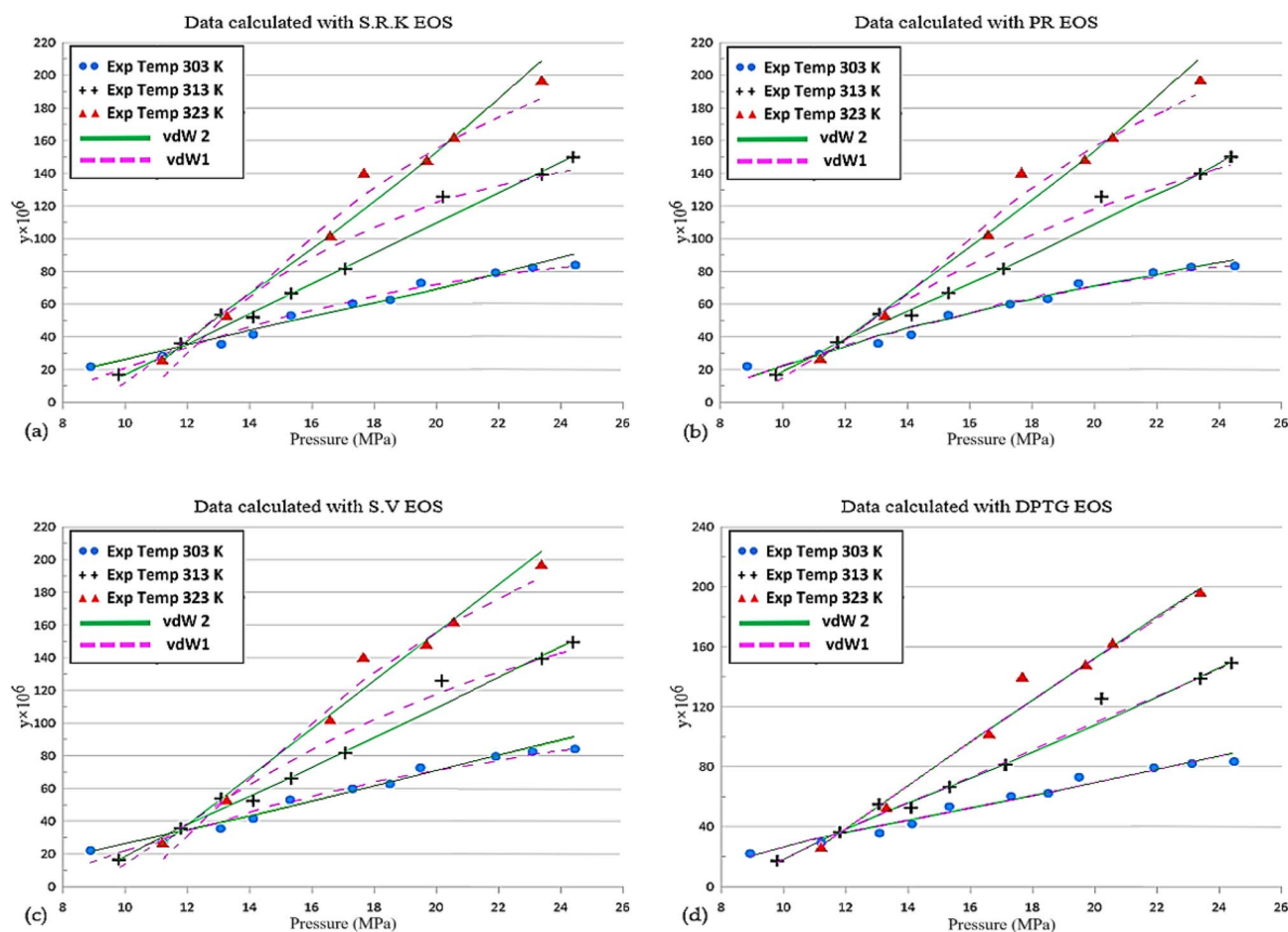


Figure 5. Comparison of experimental data (points) and calculated (line) solubility of vitamin A.

According to Fig. 4, it is implied that the growth of solubility of such compound is made through the enhancement of pressure at constant temperature. The same influence is contributed by enhancing the temperature at fixed pressure.

In such conditions, the solubility of Vitamin A is successfully represented by the chosen set of equations. Figure 5 illustrates the outcomes of AARD% according to the application of the (SRK, PR, SV and DPTG) EOSs^{17–20}.

It is revealed that achievement of adjustable parameters is possible to estimate for wide pressure ranges. This figure likewise demonstrates that the assumption of the vdW2 mixing rules to gain consistent outcomes for the solubility of Vitamin A as a compromise has been obtained at a temperature range of 303–323 K for the parameters of the objective function.

Evidently, the two correlation parameters of k_{12} and l_{12} are properly extracted that the temperature reliance on the aforementioned parameters considered by means of the fitting procedure.

EOS	Interaction parameter			
	k_{ij}		l_{ij}	
	A	B	C	D
SRK-vdW1	0.0044	-1.2581	-	-
SRK-vdW2	-0.0015	1.0655	0.0003	0.4563
PR-vdW1	0.0545	-16.619	-	-
PR-vdW2	0.0201	-5.8666	0.0228	-6.7379
SV-vdW1	0.0039	-1.1045	-	-
SV-vdW2	-0.004	1.8142	-0.0039	1.7318
DPTGvdW1	-0.0003	0.4355	-	-
DPTG-vdW2	0.0005	0.199	-0.0109	3.5373

Table 4. Adjustable parameters determined by linear regression fitting.

Holistically, DTPG EOS²⁰ with vdW2 as mixing rule were capable of relating the solubility data of Vitamin A in SC-CO₂ with the higher exactness in comparison with other EOSs.

The binary interaction parameters (k_{ij} and l_{ij}) for the vdW1 and vdW2 mixing rules are linear functions of temperature as the following:

$$k_{ij} = A_1T + A_2 \quad (20)$$

$$l_{ij} = A_3T + A_4 \quad (21)$$

In which the coefficients A_1, A_2, A_3, A_4 were assessed through the analysis of linear regression (Table 4). These linear equations are appropriate to relate the interaction parameters for assessing the solubility of Vitamin A in SC-CO₂ within the operating temperature range. Such linear equations are suitable to transmit the interface bounds for measuring the solubility of Vitamin A in SC-CO₂ in the functioning temperature range. The consequences specified that the interaction parameter of k_{ij} and l_{ij} are linearly reliant on temperature in reverse.

Conclusion

Experimental measurement of fat-soluble Vitamin A in SC-CO₂ from retinol (with 95% purification as a raw material) carried out from 303 to 323 K and at pressures from 90 to 235 bar. In this regard, solubility of Vitamin A (S (g/L)) and mole fractions (y) dissolved in SC-CO₂ were in the variety of 0.096 to 1.036 and 2.18×10^{-5} to 1.964×10^{-4} , respectively. The results were shown in Fig. 3, indicated the solubility dependency towards the variation of temperature and density. Also, with the density increases, the solubility of all substances increases at constant temperature. As long as the density remained constant, the solubility is increased resulting from the temperature increment although the improvement in the solid vapor pressure is caused by it. According to the results, the range of 0.7 g/kg was the one at which the solubility of fat-soluble vitamin A was measured in SC-CO₂ under certain conditions. For fitting curves onto the solubility data of Vitamin A compound in SC-CO₂, comparative studies were assumed so as to examine the employment of numerous cubic equations of state (SRK, PR, SV and DTPG)^{17–20} by various mixing rules (vdW1 and vdW2). Regressing the model against experimental solubility data was applied to find the optimized values of the model parameters. In the range of operating condition, 27 experimental data points were utilized for the thermodynamic equilibrium calculations.

As observed, applying DTPG EOS²⁰ and VdW2 mixing rule directs to not as much complete average relative deviation (AARD 6%) of the outcomes from the consistent experimental values in comparison with others being capable of the higher accuracy in the Vitamin A solubility data in SC-CO₂.

Received: 18 April 2021; Accepted: 9 June 2021

Published online: 05 August 2021

References

1. Sudfeld, C. R., Navar, A. M. & Halsey, N. A. Effectiveness of measles vaccination and vitamin A treatment. *Int. J. Epidemiol.* **39**(suppl_1), i48–i55. <https://doi.org/10.1093/ije/dyq021> (2010).
2. West, K. P. & Darnton-Hill, I. Vitamin A deficiency. In *Nutrition and Health in Developing Countries* (eds Semba, R. D. & Bloem, M. W.) 377–433 (Springer, 2008). https://doi.org/10.1007/978-1-59745-464-3_13.
3. Pinkaew, S. *et al.* Triple-fortified rice containing vitamin A reduced marginal vitamin A deficiency and increased vitamin A liver stores in school-aged Thai children. *J. Nutr.* **144**(4), 519–524. <https://doi.org/10.3945/jn.113.182998> (2014).
4. Pereira, C. G. & Meireles, M. A. A. Supercritical fluid extraction of bioactive compounds: fundamentals, applications and economic perspectives. *Food Bioprocess Technol.* **3**(3), 340–372. <https://doi.org/10.1007/s11947-009-0263-2> (2010).
5. Mendes, M. F., Pessoa, F. L. P. & Uller, A. M. C. An economic evaluation based on an experimental study of the vitamin E concentration present in deodorizer distillate of soybean oil using supercritical CO₂. *J. Supercrit. Fluids* **23**(3), 257–265. [https://doi.org/10.1016/S0896-8446\(01\)00140-1](https://doi.org/10.1016/S0896-8446(01)00140-1) (2002).

6. Zougagh, M., Bouabdallah, M., Salghi, R., Hormatallah, A. & Rios, A. Supercritical fluid extraction as an on-line clean-up technique for rapid amperometric screening and alternative liquid chromatography for confirmation of paraquat and diquat in olive oil samples. *J. Chromatogr. A* **1204**(1), 56–61. <https://doi.org/10.1016/j.chroma.2008.07.087> (2008).
7. Turner, C., King, J. W. & Mathiasson, L. Supercritical fluid extraction and chromatography for fat-soluble vitamin analysis. *J. Chromatogr. A* **936**(1–2), 215–237. [https://doi.org/10.1016/S0021-9673\(01\)01082-2](https://doi.org/10.1016/S0021-9673(01)01082-2) (2001).
8. Pishnamazi, M. *et al.* Measuring solubility of a chemotherapy-anti cancer drug (busulfan) in supercritical carbon dioxide. *J. Mol. Liq.* **317**, 113954. <https://doi.org/10.1016/j.molliq.2020.113954> (2020).
9. Saykhedkar, S. S. & Singhal, R. S. Supercritical carbon dioxide extraction of griseofulvin from the solid matrix obtained after solid-state fermentation. *Biotechnol. Prog.* **20**(3), 818–824. <https://doi.org/10.1021/bp0343559> (2004).
10. Brennecke, J. F. & Eckert, C. A. Phase equilibria for supercritical fluid process design. *AIChE J.* **35**(9), 1409–1427. <https://doi.org/10.1002/aic.690350902> (1989).
11. Jouyban, A., Khoubnasabjafari, M. & Chan, H.-K. Modeling the entrainer effects on solubility of solutes in supercritical carbon dioxide. *Chem. Pharm. Bull.* **53**(3), 290–295. <https://doi.org/10.1248/cpb.53.290> (2005).
12. Sodeifian, G., Hazaveie, S. M., Sajadian, S. A. & Saadati Ardestani, N. Determination of the solubility of the repaglinide drug in supercritical carbon dioxide: experimental data and thermodynamic modeling. *J. Chem. Eng. Data* **64**(12), 5338–5348. <https://doi.org/10.1021/acs.jced.9b00550> (2019).
13. Essien, S. O., Young, B. & Baroutian, S. Recent advances in subcritical water and supercritical carbon dioxide extraction of bioactive compounds from plant materials. *Trends Food Sci. Technol.* **97**, 156–169. <https://doi.org/10.1016/j.tifs.2020.01.014> (2020).
14. Pitzer, K. S. The volumetric and thermodynamic properties of fluids. I. Theoretical basis and virial coefficients I. *J. Am. Chem. Soc.* **77**(13), 3427–3433. <https://doi.org/10.1021/ja01618a001> (1955).
15. Sodeifian, G., Ardestani, N. S. & Sajadian, S. A. Solubility measurement of a pigment (Phthalocyanine green) in supercritical carbon dioxide: Experimental correlations and thermodynamic modeling. *Fluid Phase Equilib.* **494**, 61–73. <https://doi.org/10.1016/j.fluid.2019.04.024> (2019).
16. Coimbra, P., Duarte, C. M. M. & De Sousa, H. C. Cubic equation-of-state correlation of the solubility of some anti-inflammatory drugs in supercritical carbon dioxide. *Fluid Phase Equilib.* **239**(2), 188–199. <https://doi.org/10.1016/j.fluid.2005.11.028> (2006).
17. Soave, G. Equilibrium constants from a modified Redlich-Kwong equation of state. *Chem. Eng. Sci.* **27**(6), 1197–1203. [https://doi.org/10.1016/0009-2509\(72\)80096-4](https://doi.org/10.1016/0009-2509(72)80096-4) (1972).
18. Peng, D. Y. & Robinson, D. B. *Industrial Engineering Chemistry Fundamentals* (American Chemical Society, 1976).
19. Stryjek, R. & Vera, J. H. PRSV2: a cubic equation of state for accurate vapor–liquid equilibria calculations. *Can. J. Chem. Eng.* **64**(5), 820–826. <https://doi.org/10.1002/cjce.5450640516> (1986).
20. Dashtizadeh, A., Pazuki, G. R., Taghikhani, V. & Ghotbi, C. A new two-parameter cubic equation of state for predicting phase behavior of pure compounds and mixtures. *Fluid Phase Equilib.* **242**(1), 19–28. <https://doi.org/10.1016/j.fluid.2006.01.005> (2006).
21. Sodeifian, G., Sajadian, S. A. & Ardestani, N. S. Determination of solubility of Aprepitant (an antiemetic drug for chemotherapy) in supercritical carbon dioxide: empirical and thermodynamic models. *J. Supercrit. Fluids* **128**, 102–111. <https://doi.org/10.1016/j.supflu.2017.05.019> (2017).
22. da Silva, M. A. V. R., Monte, M. J. S. & Ribeiro, J. R. Vapour pressures and the enthalpies and entropies of sublimation of five dicarboxylic acids. *J. Chem. Thermodyn.* **31**(8), 1093–1107. <https://doi.org/10.1006/jcht.1999.0522> (1999).
23. Chickos, J. S. & Acree, W. E. Jr. Enthalpies of sublimation of organic and organometallic compounds. 1910–2001. *J. Phys. Chem. Ref. Data* **31**(2), 537–698. <https://doi.org/10.1063/1.1475333> (2002).
24. Ferri, A., Banchemo, M., Manna, L. & Sicardi, S. A new correlation of solubilities of azoic compounds and anthraquinone derivatives in supercritical carbon dioxide. *J. Supercrit. Fluids* **32**(1–3), 27–35. <https://doi.org/10.1016/j.supflu.2003.12.013> (2004).
25. Jin, J., Wang, Y., Zhang, Z. & Liu, H. Solubilities of benzene sulfonamide in supercritical CO₂ in the absence and presence of cosolvent. *Thermochim. Acta* **527**, 165–171. <https://doi.org/10.1016/j.tca.2011.10.023> (2012).
26. C. L. Yaws, “Vapor pressure,” in *Handbook of Chemical Compound Data for Process Safety*, Elsevier, 1997, pp. 27–53.
27. Nasri, L., Bensaad, S. & Bensetiti, Z. Correlation and prediction of the solubility of solid solutes in chemically diverse supercritical fluids based on the expanded liquid theory. *Adv. Chem. Eng. Sci.* <https://doi.org/10.4236/aces.2013.34033> (2013).
28. Prausnitz, J. M., Lichtenthaler, R. N. & De Azevedo, E. G. *Molecular Thermodynamics of Fluid-Phase Equilibria* (Pearson Education, 1998).
29. Walas, S. M. *Phase Equilibria in Chemical Engineering* (Butterworth-Heinemann, 2013).
30. Hamad, E. Z. & Yahaya, G. O. Volume-explicit equation of state and phase behavior for mixtures of hard disks. *Fluid Phase Equilib.* **168**(1), 59–69. [https://doi.org/10.1016/S0378-3812\(99\)00323-4](https://doi.org/10.1016/S0378-3812(99)00323-4) (2000).
31. Hu, J., Duan, Z., Shi, X. & Zhu, J. A general local composition and coordination number model for square-well fluids with variable well width and diameter ratio. *Mol. Phys.* **105**(8), 1019–1037. <https://doi.org/10.1080/00268970701262900> (2007).
32. Span, R. & Wagner, W. A new equation of state for carbon dioxide covering the fluid region from the triple-point temperature to 1100 K at pressures up to 800 MPa. *J. Phys. Chem. Ref. Data* **25**(6), 1509–1596. <https://doi.org/10.1063/1.555991> (1996).
33. Sodeifian, G., Sajadian, S. A. & Daneshyan, S. Preparation of Aprepitant nanoparticles (efficient drug for coping with the effects of cancer treatment) by rapid expansion of supercritical solution with solid cosolvent (RESS-SC). *J. Supercrit. Fluids* **140**, 72–84. <https://doi.org/10.1016/j.supflu.2018.06.009> (2018).
34. Khimeche, K. *et al.* Solubility of diamines in supercritical carbon dioxide: experimental determination and correlation. *J. Supercrit. Fluids* **41**(1), 10–19 (2007).
35. Perrotin-Brunel, H. *et al.* Solubility of Δ^9 -tetrahydrocannabinol in supercritical carbon dioxide: Experiments and modeling. *J. Supercrit. Fluids* **52**(1), 6–10 (2010).
36. Sodeifian, G., Sajadian, S. A. & Daneshyan, S. Preparation of Aprepitant nanoparticles (efficient drug for coping with the effects of cancer treatment) by rapid expansion of supercritical solution with solid cosolvent (RESS-SC). *J. Supercrit. Fluids* **140**, 72–84 (2018).
37. Stryjek, R. & Vera, J. H. PRSV: An improved Peng–Robinson equation of state for pure compounds and mixtures. *Can. J. Chem. Eng.* **64**(2), 323–333 (1986).

Author contributions

All authors contributed equally to this work.

Competing interests

The authors declare no competing interests.

Additional information

Supplementary Information The online version contains supplementary material available at <https://doi.org/10.1038/s41598-021-92374-x>.

Correspondence and requests for materials should be addressed to M.Z.P.

Reprints and permissions information is available at www.nature.com/reprints.

Publisher's note Springer Nature remains neutral with regard to jurisdictional claims in published maps and institutional affiliations.



Open Access This article is licensed under a Creative Commons Attribution 4.0 International License, which permits use, sharing, adaptation, distribution and reproduction in any medium or format, as long as you give appropriate credit to the original author(s) and the source, provide a link to the Creative Commons licence, and indicate if changes were made. The images or other third party material in this article are included in the article's Creative Commons licence, unless indicated otherwise in a credit line to the material. If material is not included in the article's Creative Commons licence and your intended use is not permitted by statutory regulation or exceeds the permitted use, you will need to obtain permission directly from the copyright holder. To view a copy of this licence, visit <http://creativecommons.org/licenses/by/4.0/>.

© The Author(s) 2021